POLITECNICO DI TORINO
Repository ISTITUZIONALE

Experimental Evaluation of Three-Dimensional Mode Shapes and Frame-Consistent Comparison with Numerical Models

Original
Experimental Evaluation of Three-Dimensional Mode Shapes and Frame-Consistent Comparison with Numerical Models / Usmanov, U., Battiato, G., Firrone, C.M.. - In: EXPERIMENTAL MECHANICS. - ISSN 0014-4851. - (2026). [10.1007/s11340-026-01375-2]

Availability:
This version is available at: 11583/3016792 since: 2026-10-19T18:04:00Z

Publisher:
Springer

Published
DOI:10.1007/s11340-026-01375-2

Terms of use:

This article is made available under terms and conditions as specified in the corresponding bibliographic description in the repository

Publisher copyright

(Article begins on next page)

04 November 2026

Experimental Mechanics
https://doi.org/10.1007/s11340-026-01375-2

RESEARCH PAPER

Experimental Evaluation of Three-Dimensional Mode Shapes and Frame-Consistent Comparison with Numerical Models

U. Usmanov[1] · **G. Battiato**[1] · **C. M. Firrone**[1]

Received: 13 May 2026 / Accepted: 17 September 2026
© The Author(s) 2026

Abstract

Background Experimental modal analysis with laser Doppler vibrometry is usually limited to the identification of mono-dimensional mode shapes, typically in the out-of-plane direction. This simplification restricts the understanding of the true three-dimensional deformation of a structure.

Objective The objective of this work is to develop an experimental–computational framework for the reconstruction of full three-dimensional mode shapes using a single scanning laser Doppler vibrometer and to establish a consistent procedure for comparison with numerical mode shapes expressed in different coordinate systems.

Methods The methodology combines frequency response function measurements obtained from three independent orientations of the tested component while maintaining a fixed laser head position. A reconstruction algorithm based on projection relations and rotation matrices is employed to recover the complete three-dimensional vibration shape, while an additional least-squares-based projection algorithm is introduced to project numerical mode shapes into the experimental reference frame. The methodology is experimentally validated on an air-compressor collector using a Polytec PSV-500 scanning laser Doppler vibrometer.

Results The reconstructed experimental three-dimensional mode shapes showed strong agreement with numerical predictions for the first three vibration modes, with Modal Assurance Criterion values of 0.93, 0.94, and 0.85, confirming strong modal correspondence.

Conclusions The proposed framework provides a cost-effective and flexible alternative to multi-head vibrometer systems for three-dimensional experimental modal analysis and enables reliable reconstruction of three-dimensional mode shapes together with consistent comparison with numerical models.

Keywords Experimental modal analysis · 3D mode shapes · Laser vibrometry · Reference frame projection · Vibration analysis

Introduction

Laser Doppler vibrometry has become an essential tool in experimental vibration analysis because it enables non-contact and spatially dense measurements of structural response. In conventional step-scanning procedures, a laser spot is moved across a predefined measurement grid and remains at each point long enough to record the vibration signal. While this approach provides reliable frequency response functions (FRFs) and mode shapes, it is often limited to the out-of-plane direction and requires long acquisition times when the measurement grid is dense or the surface area is large.

To overcome these limitations, more advanced scanning strategies and multi-axis vibrometer systems have been developed to capture richer information about structural vibrations [1–4]. Nevertheless, in most experimental modal analysis campaigns, the evaluation of mode shapes remains essentially one-dimensional, neglecting in-plane components that are critical to fully understanding the dynamic behavior of complex structures. This restriction limits the accuracy of model validation and the reliability of predictive simulations.

In experimental practice, the extraction of complete three-dimensional vibration information remains challenging. A single scanning laser Doppler vibrometer (SLDV) is inherently

G. Battiato is a member of SEM.

✉ U. Usmanov
umidjon.usmanov@polito.it

[1] Department of Mechanical and Aerospace Engineering, Polytechnic University of Turin, 10129 Turin, Italy

Published online: 14 October 2026

limited, as it can only capture vibration along its line of sight and therefore cannot simultaneously measure both in-plane and out-of-plane components. To overcome this limitation, commercial three-dimensional SLDV systems have been developed, such as the Polytec PSV-400-3D, PSV-500-3D and PSV QTec 3D [5]. These systems employ three scanning heads that synchronously direct laser beams to the same measurement point, allowing the full vibration vector to be reconstructed within a defined measurement coordinate system. Weisbecker et al. [6] demonstrated the capabilities of such systems for non-contact dynamic strain measurement, using a 3D scanning laser vibrometer to measure three-dimensional surface displacements from which dynamic strain fields were derived. Besides laser vibrometry, digital image correlation (DIC) has been extensively investigated as a non-contact optical technique for experimental modal characterization. Ha et al. [7] applied three-dimensional DIC to an artificial wing, demonstrating the extraction of full modal parameters, including natural frequencies, damping factors, and mode shapes. Warburton et al. [8] proposed a low-cost DIC vibrometry approach based on conventional cameras and stroboscopic illumination, reconstructing vibration deflected shapes from full-field displacement measurements and obtaining good agreement with finite element predictions. Rizo-Patron and Sirohi [9] extended the application of DIC to operational modal analysis of a rotating helicopter blade, identifying natural frequencies and mode shapes from measured bending deformations and validating them against a finite element model.

Among the most relevant contributions to three-dimensional vibration measurement is the first-time work of Chen and Zhu, who investigated the use of a three-head SLDV system operating in a continuous and synchronous scanning mode [10]. In their study, three independent vibrometer heads (Top, Left, and Right) were arranged to simultaneously track the same point along a prescribed trajectory on the surface of the structure. By synchronizing the scanning paths of all three beams, the system was able to record vibration components along three distinct laser directions. However, this methodology depends on the availability of a specialized 3D-SLDV system, such as the Polytec PSV-500-3D, which integrates multiple scanning heads into a single measurement platform. While technically powerful, the cost of such equipment is extremely high, often exceeding the budget available in many academic or industrial laboratories. In addition, the physical space required to install and calibrate three independent laser heads can make the method impractical in certain test environments, particularly when the geometry of the component restricts the access. Another work proposed by the same authors investigate three-dimensional vibration measurement using a single SLDV [11]. In their work, the SLDV is sequentially repositioned at three distinct locations, and the vibration components along a predefined measurement coordinate system are reconstructed by combining the velocity projections measured along different laser directions. However, the physical relocation of the vibrometer introduces additional experimental complexity, as it requires accurate repositioning of the measurement point across successive acquisitions. Moreover, the approach relies on precise geometric calibration and consistent positioning, which may influence the accuracy of the reconstructed components.

The present work addresses this limitation through a different experimental and computational formulation. In the current framework, the scanning head remains fixed throughout the measurement campaign and the tested component is sequentially reoriented into three spatial configurations. The methodological contribution is a formulation of a fixed-SLDV, specimen-reorientation framework specifically integrated with experimental modal analysis. The frequency response functions (FRFs) extracted from these separate tests are then utilized through a dedicated algorithm to reconstruct the complete three-dimensional mode shapes. This strategy significantly reduces instrumentation costs and expands the applicability of 3D experimental modal analysis to a broader range of laboratories and test setups. While it requires sequential rather than simultaneous measurements, the approach preserves the essential capability of identifying full 3D mode shapes, thus offering a practical and cost-effective alternative to multi-head vibrometer systems. In addition, a reference-frame alignment procedure is introduced to project numerical mode shapes into the experimental coordinate system, enabling direct comparison and MAC-based validation of the reconstructed modes. The proposed framework therefore extends single-SLDV three-dimensional vibration measurement from point-wise reconstruction toward a practical workflow for full-field experimental modal identification and numerical–experimental correlation.

Methodology

The starting point of the proposed methodology is the definition of how a scanning laser Doppler vibrometer (SLDV) records the motion of a vibrating point. Figure 1 shows the schematic representation of the measurement principle. Let point C be located on the surface of the structure. Its motion is described with respect to a user-defined Cartesian reference frame (x,y,z). This reference frame is body fixed and can be arbitrarily chosen by the operator and will be referred to as the experimental reference frame throughout the paper. The SLDV is positioned at point E, and its orientation relative to the experimental frame is described by two inclination angles: the horizontal angle β and the vertical angle α. These angles represent the deviation of the laser beam from the normal direction to the measured surface. Depending on the instrument type, the velocity measured by the vibrometer can

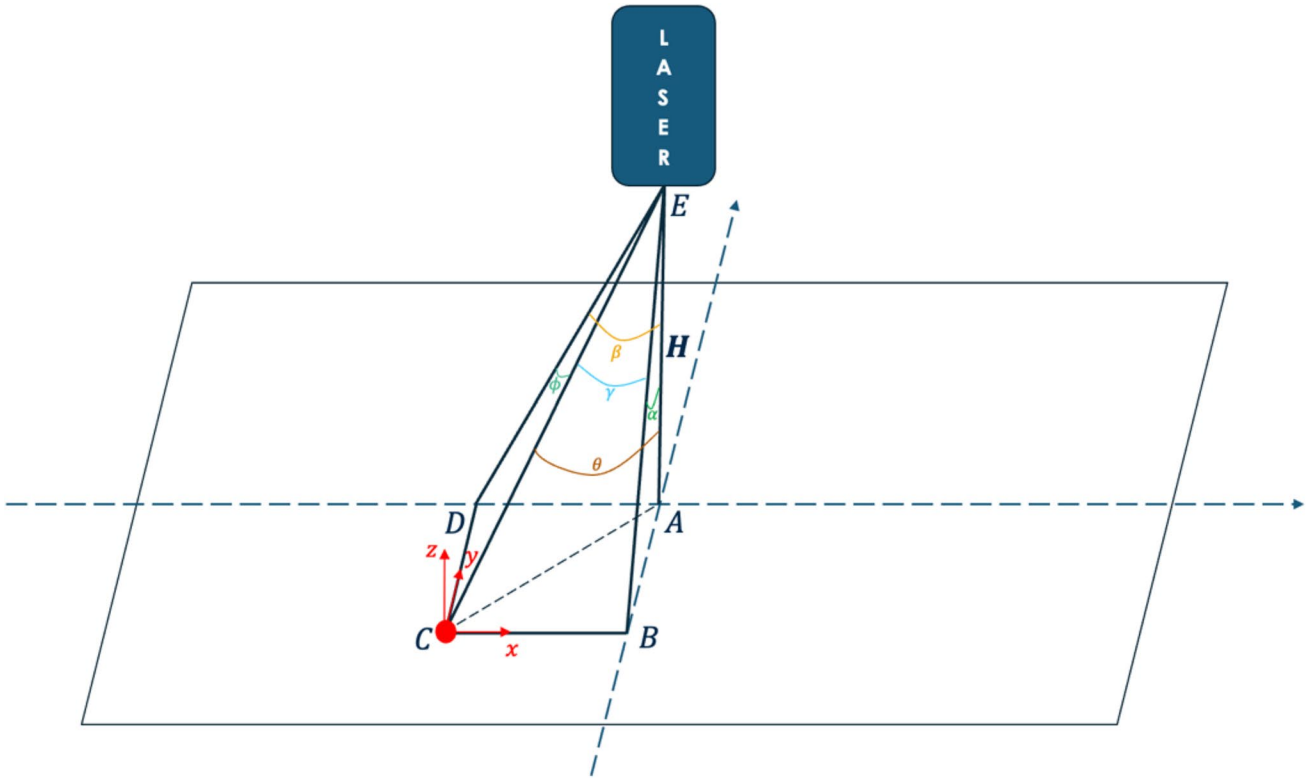


Fig. 1 Laser vibrometer measurement scheme in the neutral configuration

be interpreted in different ways. In the most general case, a mono-dimensional vibrometer provides the projection of the velocity vector along the laser beam axis, i.e., along the line *EC*. This direction usually does not coincide with any axis of the experimental reference frame. For this reason, the raw measurement cannot be directly assigned to in-plane or out-of-plane vibration components. Some commercial vibrometers incorporate internal correction algorithms that account for the inclination of the laser head. In these cases, the system outputs the velocity component aligned with the out-of-plane direction of the measured surface, which in our notation corresponds to the z-axis. While this feature simplifies the interpretation of the measurements, it is not universally available, and its implementation varies between instruments.

The methodology proposed in this work follows a generic formulation that assumes the vibrometer does not perform such corrections. Accordingly, the measured signal is always considered as the projection of the velocity vector along the laser line. This general assumption allows the derivation of a set of equations that remain valid independently of the specific instrument. For users employing a vibrometer with built-in correction, the same formulation can be recovered by setting the inclination angles to zero, i.e., $\alpha = 0$ and $\beta = 0$. In this way, the proposed methodology provides a unified framework that can be applied both to corrected and uncorrected vibrometer outputs.

The experimental reference frame *(x,y,z)* is the basis in which all reconstructed 3D mode shapes are expressed. The SLDV records the projection of the motion of point *C* onto a laser line beam direction. By applying simple trigonometric relations to triangles *ECB*, *EDC* and *ECA* in Fig. 1, the laser reading *LR* of the point *C* can be expressed as

$$LR = v_x \sin\gamma + v_y \sin\phi + v_z \cos\theta \tag{1}$$

where v_x, v_y and v_z are velocity components in the experimental reference frame. Since only the inclination angles α and β are typically available to the user from the laser equipment, it is necessary to express the beam projection angles γ, ϕ and θ in terms of α and β. The relations can be obtained by applying elementary trigonometric identities to the right-angled triangles *EAB, EBC, EDC* and *EAC* shown in Fig. 1. The resulting expressions are

$$\sin\gamma = \frac{\tan\beta \cdot \cos\alpha}{\sqrt{1+\cos^2\alpha \cdot \tan^2\beta}}; \sin\phi = \frac{\sin\alpha}{\sqrt{1+\cos^2\alpha \cdot \tan^2\beta}}; \cos\theta = \frac{\cos\alpha}{\sqrt{1+\cos^2\alpha \cdot \tan^2\beta}} \tag{2}$$

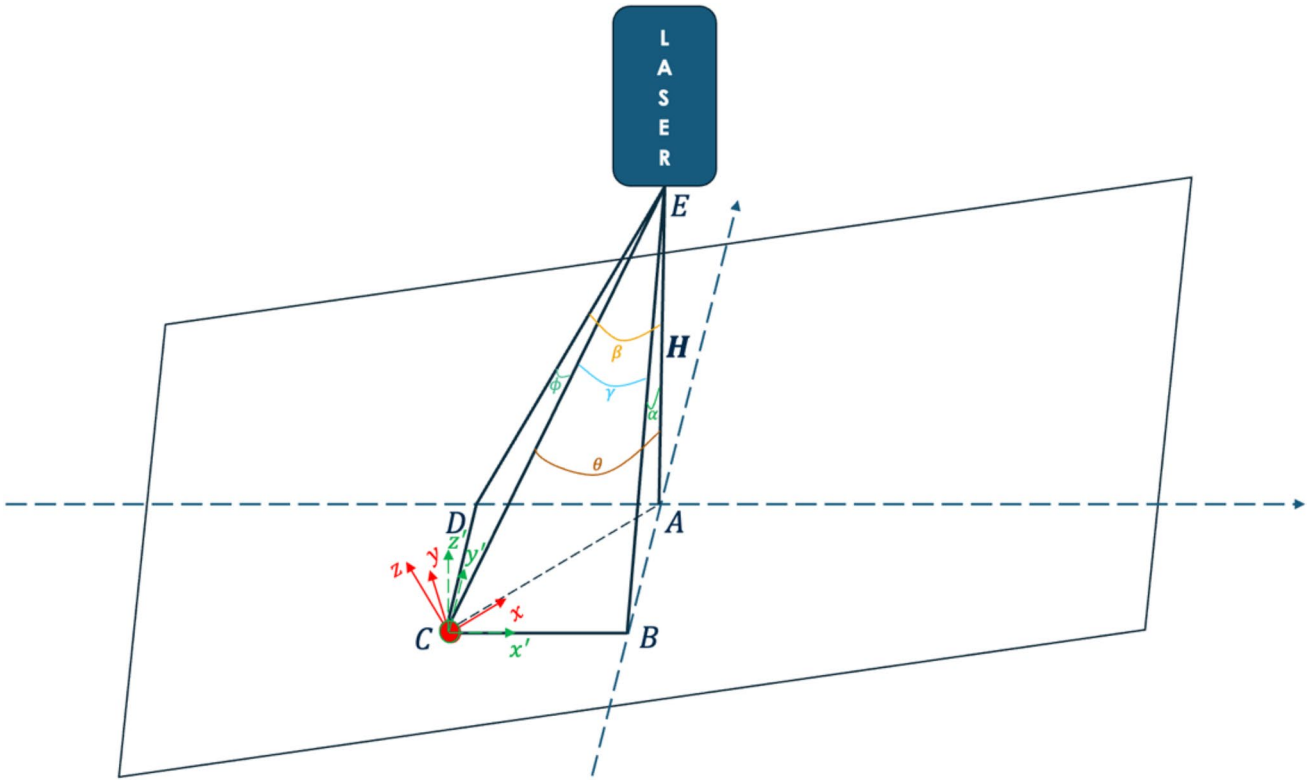


Fig. 2 Laser vibrometer measurement scheme in a rotated configuration

By substituting these trigonometric relations into the expression of laser reading (Eq. 1), the projection can be compactly written as

$$LR = \frac{1}{\sqrt{1+\cos^2\alpha \cdot \tan^2\beta}} \left[\tan\beta \cdot \cos\alpha \;\; \sin\alpha \;\; \cos\alpha\right] \begin{Bmatrix} v_x \\ v_y \\ v_z \end{Bmatrix} \tag{3}$$

It is important to note that, in the special case where the vibrometer performs an internal correction of the inclination angles ($\alpha = 0$ and $\beta = 0$), the projection reduces to $LR = v_z$, which corresponds to the direct measurement of the pure out-of-plane motion of the component.

Since our goal is to recover the motion vector $\{v_x, v_y, v_z\}^T$, a single laser reading provides only one scalar projection, so the problem is underdetermined (three unknowns and one equation). To solve a system, we repeat measurement under at least three independent configurations. In practice, this is achieved by reorienting the component (e.g. rotating it about one or more axis), while the laser head remains fixed. Figure 2 depicts a generic re-orientation of the specimen. Vibrometer has no information about how the component is rotated, the output of the vibrometer still refers to the original experimental frame defined at the beginning of the test. In the scheme, this is shown as the green frame (x',y',z'). For consistency, however, the vibration results must be expressed in the body-fixed frame that follows the orientation of the component ((x,y,z) in Fig. 2). This requires introducing a transformation that accounts for the relative rotation between the experimental reference frame and the rotated body frame. Any generic rotation of the component can be represented as a sequence of three consecutive rotations about the principal axes of the experimental reference frame. This is commonly referred as the Euler rotation formalism. In this framework, a rotation about the z-axis by an angle δ_z, followed by a rotation about the y-axis by δ_y, and finally a rotation about the x-axis by δ_x, transforms the original reference frame (x,y,z) into the rotated frame (x',y',z'):

$$\boldsymbol{R}_{rot} = \boldsymbol{R}_x\boldsymbol{R}_y\boldsymbol{R}_z = \begin{bmatrix} \cos\delta_z & \sin\delta_z & 0 \\ -\sin\delta_z & \cos\delta_z & 0 \\ 0 & 0 & 1 \end{bmatrix}\begin{bmatrix} 1 & 0 & 0 \\ 0 & \cos\delta_x & \sin\delta_x \\ 0 & -\sin\delta_x & \cos\delta_x \end{bmatrix}\begin{bmatrix} \cos\delta_y & 0 & -\sin\delta_y \\ 0 & 1 & 0 \\ \sin\delta_y & 0 & \cos\delta_y \end{bmatrix} = \begin{bmatrix} \cos\delta_y\cos\delta_z & \cos\delta_y\sin\delta_z & -\sin\delta_y \\ \sin\delta_x\sin\delta_y\cos\delta_z - \cos\delta_x\sin\delta_z & \sin\delta_x\sin\delta_y\sin\delta_z + \cos\delta_x\cos\delta_z & \sin\delta_x\cos\delta_y \\ \cos\delta_x\sin\delta_y\cos\delta_z + \sin\delta_x\sin\delta_z & \cos\delta_x\sin\delta_y\sin\delta_z - \sin\delta_x\cos\delta_z & \cos\delta_x\cos\delta_y \end{bmatrix} \tag{4}$$

With the three independent configurations, the three laser readings provide three independent projections of the same motion at point *C*. Stacking these relations yield a 3 by 3 linear system for the unknown component $\{v_x, v_y, v_z\}^T$.

$$\begin{cases} LR_1 = \frac{1}{\sqrt{1+\cos^2\alpha_1 \cdot \tan^2\beta_1}} \left[\tan\beta_1 \cdot \cos\alpha_1 \;\; \sin\alpha_1 \;\; \cos\alpha_1 \right] \cdot R_{rot,1} \cdot \begin{Bmatrix} v_x \\ v_y \\ v_z \end{Bmatrix} \\ LR_2 = \frac{1}{\sqrt{1+\cos^2\alpha_2 \cdot \tan^2\beta_2}} \left[\tan\beta_2 \cdot \cos\alpha_2 \;\; \sin\alpha_2 \;\; \cos\alpha_2 \right] \cdot R_{rot,2} \begin{Bmatrix} v_x \\ v_y \\ v_z \end{Bmatrix} \\ LR_3 = \frac{1}{\sqrt{1+\cos^2\alpha_3 \cdot \tan^2\beta_3}} \left[\tan\beta_3 \cdot \cos\alpha_3 \;\; \sin\alpha_3 \;\; \cos\alpha_3 \right] \cdot R_{rot,3} \cdot \begin{Bmatrix} x \\ y \\ z \end{Bmatrix} \end{cases} \tag{5}$$

$$\begin{Bmatrix} LR_1 \\ LR_2 \\ LR_3 \end{Bmatrix} = \boldsymbol{T} \cdot \begin{Bmatrix} v_x \\ v_y \\ v_z \end{Bmatrix} \tag{6}$$

This system can be directly solved through matrix inversion, since the transformation matrix $\boldsymbol{T}$ is non-singular and well-conditioned as long as the three projection directions are not coplanar or nearly collinear. In practice, this condition is satisfied by choosing distinct rotations in the range of 20–45°. Under such conditions, the inversion is numerically stable and provides the three vibration components $\{v_x, v_y, v_z\}^T$. If more than three configurations are available, the system becomes overdetermined, and the unknowns can be estimated in a least-squares sense, which improves robustness against measurement noise and experimental uncertainties.

$$\begin{Bmatrix} v_x \\ v_y \\ v_z \end{Bmatrix} = T^{-1} \begin{Bmatrix} LR_1 \\ LR_2 \\ LR_3 \end{Bmatrix} \tag{7}$$

The second part of this work addresses the challenge of comparing experimentally reconstructed mode shapes with numerical predictions. In many cases, finite element (numeric) mode shapes are defined with respect to a numerical reference frame that does not coincide with the experimental frame used during measurements. For simple geometries, the relation between these frames can often be established analytically. However, for components with complex geometry, the relation between the numerical and experimental reference frames is not straightforward and cannot be easily derived. The relation between the mode shape defined in numerical and experimental reference frame can be written in terms of the rotation matrix R_{num}:

$$\begin{Bmatrix} v_x \\ v_y \\ v_z \end{Bmatrix}_{exp} = \boldsymbol{R}_{num} \begin{Bmatrix} v_x \\ v_y \\ v_z \end{Bmatrix}_{num} \tag{8}$$

the transformation between the numerical and experimental reference frames can be described by a single rotation matrix, denoted $\boldsymbol{R}_{num}$. This matrix is of size 3×3 and defines how the numerical coordinates $\left(v_x, v_y, v_z\right)^T_{num}$ are rotated in order to align with the experimental coordinates $\left(v_x, v_y, v_z\right)^T_{exp}$. For each measurement point of the component, the same rotation applies, meaning that the transformation is consistent across the entire structure. When the mode shape vector is written for all measurement points, the global transformation matrix takes a block-diagonal form. Each block is identical and equal to $\boldsymbol{R}_{num}$, while the size of the full matrix scales with the number of measurement points. In this way, the entire numerical mode shape can be projected into the experimental frame simply by applying this block-diagonal transformation:

$$\begin{Bmatrix} v_{x1} \\ v_{y_1} \\ v_{z_1} \\ v_{x2} \\ v_{y_2} \\ v_{z2} \\ \vdots \\ v_{xn} \\ v_{y_n} \\ v_{zn} \end{Bmatrix}_{exp} = \begin{bmatrix} R_{11} & R_{12} & R_{13} & 0 & 0 & 0 & \cdots & 0 & 0 & 0 \\ R_{21} & R_{22} & R_{23} & 0 & 0 & 0 & \cdots & 0 & 0 & 0 \\ R_{31} & R_{32} & R_{33} & 0 & 0 & 0 & \cdots & 0 & 0 & 0 \\ 0 & 0 & 0 & R_{11} & R_{12} & R_{31} & \cdots & 0 & 0 & 0 \\ 0 & 0 & 0 & R_{21} & R_{22} & R_{23} & \cdots & 0 & 0 & 0 \\ 0 & 0 & 0 & R_{31} & R_{32} & R_{33} & \cdots & 0 & 0 & 0 \\ \vdots & \vdots & \vdots & \vdots & \vdots & \vdots & \ddots & 0 & 0 & 0 \\ 0 & 0 & 0 & 0 & 0 & 0 & \cdots & R_{11} & R_{12} & R_{13} \\ 0 & 0 & 0 & 0 & 0 & 0 & \cdots & R_{21} & R_{22} & R_{32} \\ 0 & 0 & 0 & 0 & 0 & 0 & \cdots & R_{31} & R_{32} & R_{33} \end{bmatrix} \cdot \begin{Bmatrix} v_{x1} \\ v_{y_1} \\ v_{z_1} \\ v_{x2} \\ v_{y_2} \\ v_{z2} \\ \vdots \\ v_{xn} \\ v_{y_n} \\ v_{zn} \end{Bmatrix}_{num} \tag{9}$$

Since the transformation matrix $\boldsymbol{R}_{num}$ is not known, the objective is to determine it. Both numerical and experimental mode shape vectors are available, expressed in their respective reference frames. By rewriting the relation between them, the numerical mode shape vector can be arranged in matrix form, while the entries of $\boldsymbol{R}_{num}$ are treated as unknowns to be solved. This formulation leads to a linear system where the coefficients come from the numerical mode shapes and the unknown vector contains the nine components of the transformation matrix:

$$\begin{Bmatrix} v_{x1} \\ v_{y_1} \\ v_{z_1} \\ v_{x2} \\ v_{y_2} \\ v_{z2} \\ \vdots \\ v_{xn} \\ v_{y_n} \\ v_{zn} \end{Bmatrix}_{exp} = \begin{bmatrix} v_{x_1} & v_{y_1} & v_{z1} & 0 & 0 & 0 & 0 & 0 & 0 \\ 0 & 0 & 0 & v_{x1} & v_{y_1} & v_{z1} & 0 & 0 & 0 \\ 0 & 0 & 0 & 0 & 0 & 0 & v_{x1} & v_{y_1} & v_{z1} \\ v_{x2} & v_{y_2} & v_{z2} & 0 & 0 & 0 & 0 & 0 & 0 \\ 0 & 0 & 0 & v_{x2} & v_{y_2} & v_{z2} & 0 & 0 & 0 \\ 0 & 0 & 0 & 0 & 0 & 0 & v_{x2} & v_{y_2} & v_{z2} \\ \vdots & \vdots & \vdots & \vdots & \vdots & \vdots & \vdots & \vdots & \vdots \\ v_{xn} & v_{y_n} & v_{z_{n,n}} & 0 & 0 & 0 & 0 & 0 & 0 \\ 0 & 0 & 0 & v_{xn} & v_{y_n} & v_{zn} & 0 & 0 & 0 \\ 0 & 0 & 0 & 0 & 0 & 0 & v_{xn} & v_{y_n} & v_{zn} \end{bmatrix}_{num} \begin{Bmatrix} R_{11} \\ R_{12} \\ R_{13} \\ R_{21} \\ R_{22} \\ R_{23} \\ R_{31} \\ R_{32} \\ R_{33} \end{Bmatrix} = V \begin{Bmatrix} R_{11} \\ R_{12} \\ R_{13} \\ R_{21} \\ R_{22} \\ R_{23} \\ R_{31} \\ R_{32} \\ R_{33} \end{Bmatrix} \tag{10}$$

This system is generally overdetermined, since multiple measurement points contribute independent equations for the same unknown transformation matrix. Therefore, the problem cannot be solved exactly but can be approached using the least squares method.

$$\begin{Bmatrix} R_{11} \\ R_{12} \\ R_{13} \\ R_{21} \\ R_{22} \\ R_{23} \\ R_{31} \\ R_{32} \\ R_{33} \end{Bmatrix} = \boldsymbol{V}^{+} \begin{Bmatrix} v_{x1} \\ v_{y1} \\ v_{z1} \\ v_{x2} \\ v_{y2} \\ v_{z2} \\ \vdots \\ v_{xn} \\ v_{yn} \\ v_{zn} \end{Bmatrix}_{exp} \tag{11}$$

Applications

The experiments were performed on a mechanical component designed to exhibit clear three-dimensional vibration behavior, in order to assess the effectiveness of the proposed algorithm. The measurements were carried out using a Poly-Tec QTec PSV-500 scanning laser Doppler vibrometer. The selected component is a collector from an air-compressor. A total of 18 measurement points were defined on its surface, as shown in Fig. 3(a).

To enable the reconstruction of the full 3D mode shapes, the component was tested in three distinct orientations with respect to the laser beam:

- Neutral position – the main plane of the component was kept orthogonal to the laser beam (Fig. 3(a)).
- Rotation about the x-axis – the component was rotated by 30° (Fig. 3(b)).
- Rotation about the y-axis – the component was rotated by 30° (Fig. 3(c)).

The chosen orientations ensured that the laser projections were sufficiently distinct, thereby providing the independent information necessary for solving the system of equations and extracting the 3D motion. The experimental reference frame used for all measurements is illustrated in Fig. 3(a).

An example of a measured frequency response function (FRF) for a single measurement point in the neutral configuration is shown in Fig. 4. Peaks in the response correspond to the resonance frequencies of the component, which are later used for mode shape extraction.

It is important to note that the laser vibrometer directly measures velocity, whereas mode shapes are commonly defined in terms of displacement. However, for a harmonic response at a given frequency, velocity and displacement are simply related by the angular frequency. This implies that the measured velocity is equal to the corresponding displacement scaled by angular frequency. Since scaling a mode shape vector does not alter its spatial distribution, the mode shapes can be evaluated directly from the velocity measurements without additional transformation.

Regarding the identification of modal parameters, the measured FRFs exhibit distinct, well-separated resonance peaks with sharp profiles, indicating low modal damping and the absence of modal coupling. Under these conditions, a simple peak-picking method was adopted for the extraction of the modal frequencies and associated mode

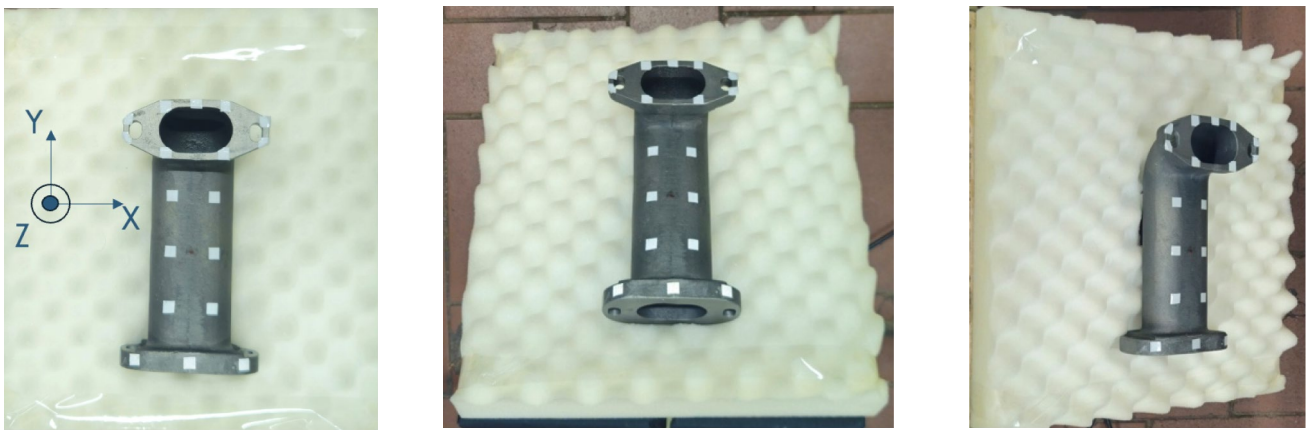


Fig. 3 Experimental setup and orientations of the tested component: (**a**) neutral position with no rotation; (**b**) rotation of 30° about the *x*-axis (YZ-plane rotation, clockwise); (**c**) rotation of 30° about the *y*-axis (XZ-plane rotation, counterclockwise)

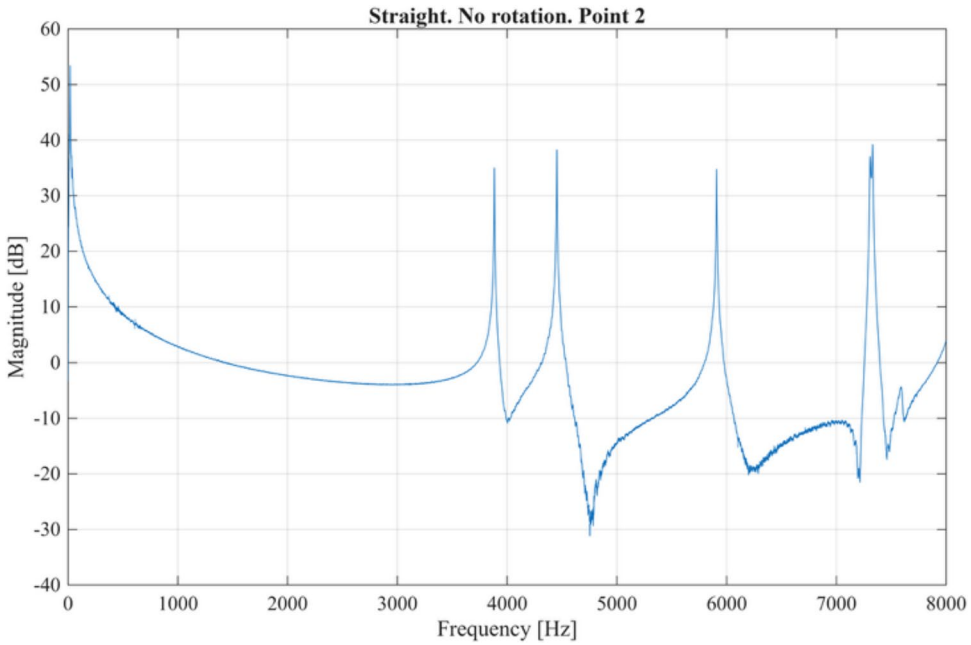


Fig. 4 An example of a measured FRF in the neutral configuration (no rotation)

shapes. For the present study, the analysis was limited to the three modes. The determination of the rotation matrix in Eq. (10–11) was carried out by employing the mode shape measurements obtained from all three identified modes. Using multiple modes in the formulation ensures consistency and improves the robustness of the estimation, as the transformation matrix must remain valid across different mode shapes of the same structure.

The comparison between experimental and numerical 3D mode shapes is presented in Fig. 5 for the first three modes. In all cases, the undeformed geometry is shown in gray, while the experimental and numerical deformed shapes are overlaid. The results indicate a very good agreement in the overall deformation patterns, with the experimental shapes closely following the numerical predictions. Small local deviations are visible at certain measurement points, which can be attributed to experimental noise and limitations in spatial resolution. Nevertheless, the global characteristics of the vibration modes are consistently reproduced.

The quality of the correlation was further assessed using the Modal Assurance Criterion (MAC), shown in Fig. 6. The diagonal values are very close to unity for all three modes (0.93, 0.94, and 0.85, respectively), confirming a strong correspondence between experimental and numerical shapes. The off-diagonal terms remain close to zero, demonstrating a clear separation between the identified modes and the absence of significant cross-correlation. These results validate the effectiveness of the proposed methodology in reconstructing experimental 3D mode shapes and provide confidence in their use for comparison against numerical predictions.

Sensitivity to Angular Misalignment Uncertainty

To further assess the robustness of the proposed reconstruction methodology, the sensitivity of the reconstructed three-dimensional mode shapes to angular alignment uncertainty was investigated through a Monte Carlo analysis. The two nominal specimen rotations used for the reconstruction were independently perturbed by angular deviations ($\boldsymbol{\Delta\theta_{YZ}}$) and ($\boldsymbol{\Delta\theta_{XZ}}$), both sampled from a uniform distribution over the interval $[-3°, +3°]$. This interval was selected to represent a conservative uncertainty associated with the manual angular positioning of the specimen. A total of 10,000 independent realizations were generated for each of the first three modes. For each realization, the corresponding rotation matrices and transformation matrix were recalculated using the perturbed angles. The resulting three-dimensional mode shape was then compared with the nominal experimental mode shape reconstructed using zero angular deviation through MAC number.

The statistical results in Table 1 indicate a limited sensitivity of the reconstructed mode shapes to the considered angular uncertainty. The mean MAC remains at or above 0.997 for all three modes, while the corresponding standard deviations are of the order of 10^{-3}. To illustrate

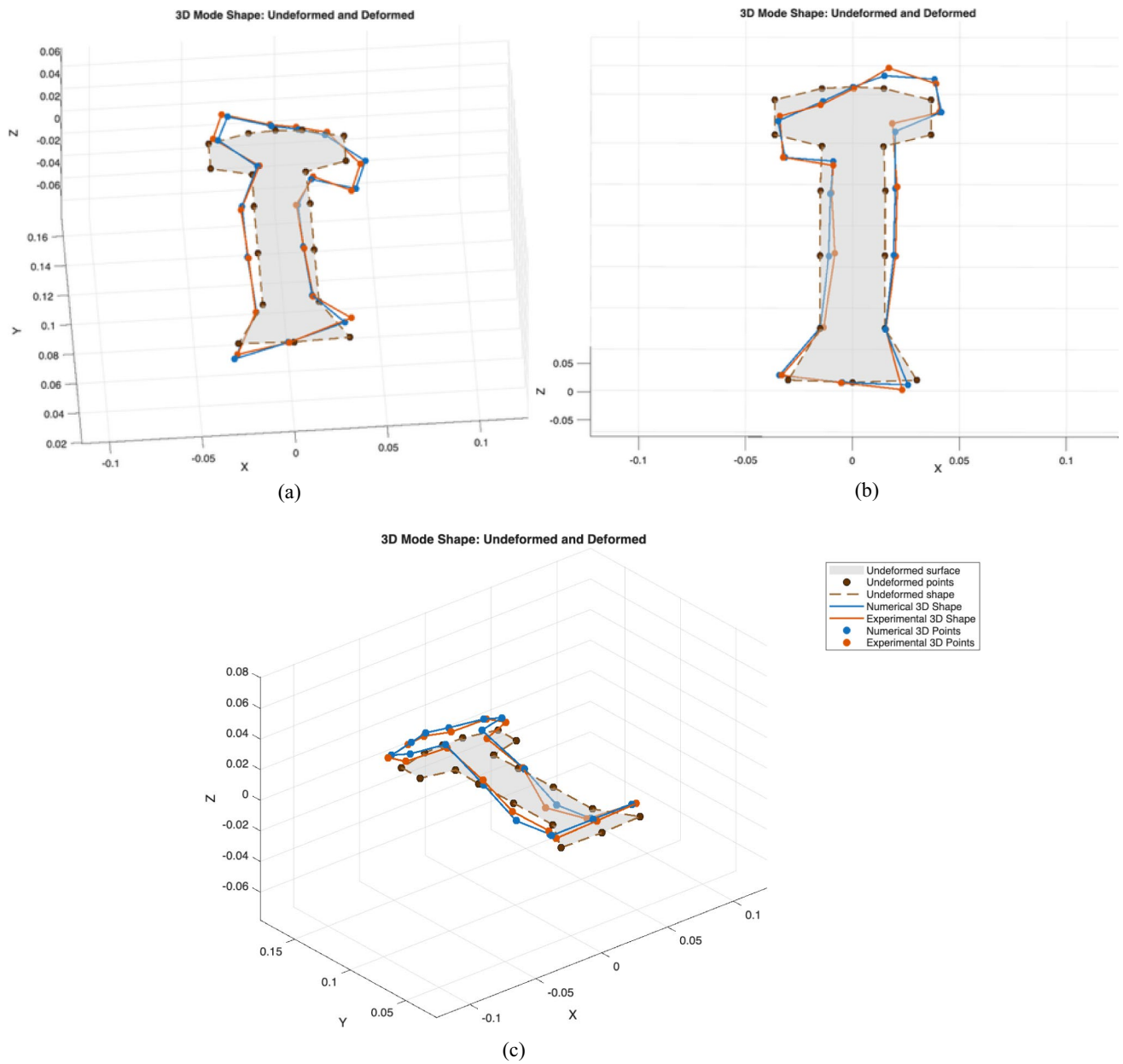


Fig. 5 Comparison of experimental and numerical 3D mode shapes for the first three modes: (**a**) Mode 1, (**b**) Mode 2, (**c**) Mode 3

the distribution and dependence on the individual angular perturbations in greater detail, the results for Mode 1 are reported in Figs. 7. Mode 1 was selected for visualization because it exhibited the largest variability and the lowest minimum MAC among the three investigated modes, thereby representing the most sensitive case.

The MAC distribution in Fig. 7(a) is strongly concentrated close to unity. Most realizations result in MAC values above approximately 0.997, while only a small fraction extends toward the minimum value of 0.990. The narrow range of the distribution confirms that the global deformation pattern of Mode 1 is only weakly affected by the considered alignment uncertainty. Figure 7(b) provides further insight into the propagation of the angular uncertainty through the reconstruction procedure. The highest MAC values are obtained in the vicinity of zero angular deviation, as expected, while the correlation gradually decreases as the magnitude of the perturbations increases. The smooth variation of the MAC over the investigated domain indicates that the reconstruction does not exhibit abrupt sensitivity to small changes in the prescribed angles. Even toward the boundaries of the considered uncertainty interval, the MAC

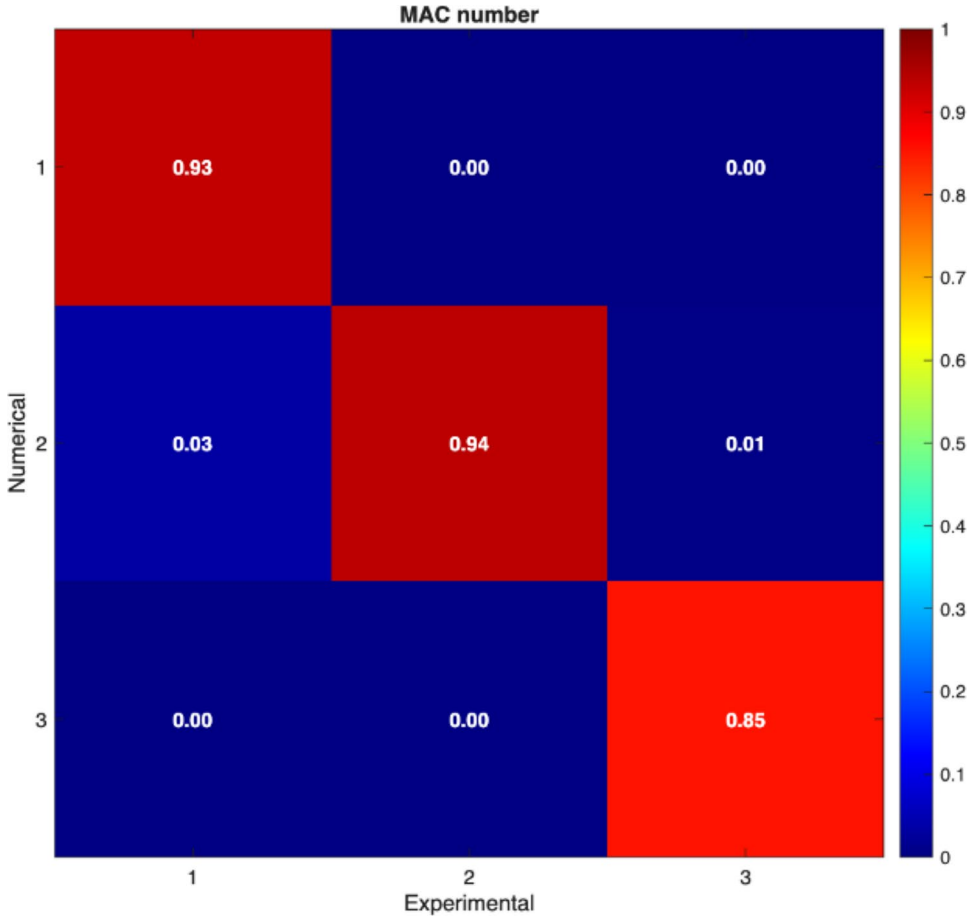


Fig. 6 Modal Assurance Criterion (MAC) matrix comparing experimental and numerical 3D mode shapes for the first three modes

Table 1 Statistical characterization of the MAC between the nominal and perturbed experimental 3D modes

Mode	Mean MAC	Standard deviation	Minimum MAC	95th percentile
1	0.997	0.001	0.99	0.99
2	0.998	0.001	0.99	0.99
3	0.998	0.001	0.99	0.99

remains approximately 0.99 or higher for Mode 1. This behavior indicates that the reconstruction error increases progressively with angular misalignment rather than being strongly amplified by the inversion procedure.

Overall, the Monte Carlo analysis demonstrates that independent angular alignment errors have only a limited influence on the reconstructed three-dimensional mode shapes. Although Fig. 7 presents the results only for Mode 1, similar distributions and sensitivity patterns were observed for Modes 2 and 3. The consistently high MAC values obtained for all three investigated modes therefore support the robustness of the proposed methodology with respect to realistic uncertainties in the angular positioning of the specimen.

Conclusion

This work has presented a novel methodology for the experimental evaluation of three-dimensional mode shapes using a single scanning laser Doppler vibrometer. Unlike conventional approaches that require multiple laser heads for simultaneous multi-directional measurements, the proposed method relies on repositioning the test component in different orientations. By combining three independent measurement configurations and applying a dedicated reconstruction algorithm, the full 3D mode shapes can be extracted. An additional algorithm was introduced to transform numerical mode shapes into the experimental reference frame, enabling a consistent and meaningful comparison between numerical predictions and experimental data even when the reference frames are not directly aligned.

The main advantages of the method are its simplicity, cost-effectiveness, and flexibility. The requirement of only one laser scanning head makes the approach accessible in laboratory environments where multi-head systems are impractical due to high cost or setup complexity. Furthermore, the framework is general and does not rely on prior knowledge of the component geometry, making it suitable for both simple and complex structures.

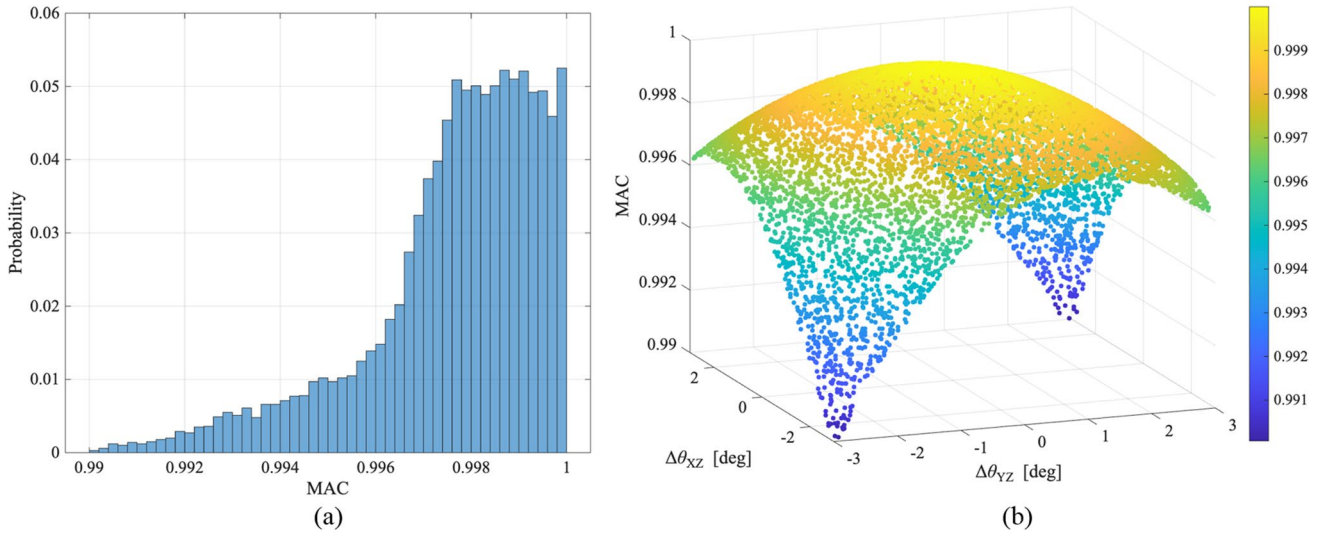


Fig. 7 Sensitivity of the reconstructed Mode 1 to angular alignment uncertainty: (**a**) probability distribution of the MAC values obtained from 10000 Monte Carlo realizations; (**b**) dependence of the MAC on the independent angular perturbations $\boldsymbol{\Delta\theta_{YZ}}$ and $\boldsymbol{\Delta\theta_{XZ}}$, uniformly distributed within $[-3°, +3°]$

The methodology was validated through experiments performed on a mechanical component exhibiting clear 3D vibration behavior. Three orientations of the component were used to generate independent measurements, from which the 3D mode shapes were reconstructed. Comparison with numerical mode shapes showed very good agreement. The overlaid mode shape plots confirmed the accuracy of the reconstructed deformation patterns, while the MAC analysis yielded high diagonal values (0.93, 0.94, and 0.85) and near-zero off-diagonal values, demonstrating strong correlation and proper mode separation. The robustness of the reconstruction against angular alignment uncertainty was further assessed through a Monte Carlo analysis with 10,000 realizations and independent angular perturbations within $\pm 3°$. Mean MAC values between the perturbed and nominal reconstructed mode shapes remained between 0.997 and 0.998 for all investigated modes, demonstrating a low sensitivity of the proposed methodology to realistic angular positioning uncertainties.

Author Contributions Umidjon Usmanov: Conceptualization, methodology, software, numerical simulations, experimental investigation, data curation, visualization, validation, writing—original draft preparation.

Giuseppe Battiato: Supervision, methodology, validation, scientific discussion, writing—review and editing.

Christian Maria Firrone: Supervision, conceptualization, project administration, scientific discussion, writing—review and editing.

All authors have read and agreed to the published version of the manuscript.

Funding Open access funding provided by Politecnico di Torino within the CRUI-CARE Agreement.

Data Availability All data supporting the findings of this study are available within the article.

Declarations

Competing interests The authors declare that they have no known competing financial interests or personal relationships that could have appeared to influence the work reported in this paper.

Open Access This article is licensed under a Creative Commons Attribution 4.0 International License, which permits use, sharing, adaptation, distribution and reproduction in any medium or format, as long as you give appropriate credit to the original author(s) and the source, provide a link to the Creative Commons licence, and indicate if changes were made. The images or other third party material in this article are included in the article's Creative Commons licence, unless indicated otherwise in a credit line to the material. If material is not included in the article's Creative Commons licence and your intended use is not permitted by statutory regulation or exceeds the permitted use, you will need to obtain permission directly from the copyright holder. To view a copy of this licence, visit http://creativecommons.org/licenses/by/4.0/.

References

1. Sriram P, Craig J (1992) Mode shape measurement using a scanning laser doppler vibrometer. Int J Anal Exp Modal Anal 7(3):169–178
2. Stanbridge A, Ewins D (1999) Modal testing using a scanning laser doppler vibrometer. Mech Syst Signal Process 13(2):255–270
3. Allen MS, Sracic MW (2010) A new method for processing impact excited continuous-scan laser doppler vibrometer measurements. Mech Syst Signal Process 24(3):721–735
4. Halkon BJ, Frizzel S, Rothberg S (2003) Vibration measurements using continuous scanning laser vibrometry: velocity sensitivity model experimental validation. Meas Sci Technol 14(6):773

5. Polytec GmbH, "PSV-500–3D Scanning Vibrometer Product Page," Polytec Vibrometry Products – Full-Field Vibrometers. https://www.polytec.com/int/vibrometry/products/full-field-vibrometers/psv-500-3d-scanning-vibrometer. Accessed August 2025
6. Weisbecker H, Cazzolato B, Wildy S et al (2012) Surface strain measurements using a 3D scanning laser vibrometer. Exp Mech 52:805–815
7. Ha NS, Vang HM, Goo NS (2015) Modal analysis using digital image correlation technique: an application to artificial wing mimicking beetle's hind wing. Exp Mech 55:989–998
8. Warburton JR, Lu G, Buss TM et al (2016) Digital image correlation vibrometry with low speed equipment. Exp Mech 56:1219–1230
9. Rizo-Patron S, Sirohi J (2017) Operational modal analysis of a helicopter rotor blade using digital image correlation. Exp Mech 57:367–375
10. Chen D-M, Zhu WD (2021) Investigation of three-dimensional vibration measurement by three scanning laser doppler vibrometers in a continuously and synchronously scanning mode. J Sound Vib 498:115950
11. Chen D-M, Zhu WD (2017) Investigation of three-dimensional vibration measurement by a single scanning laser doppler vibrometer. J Sound Vib 387:36–52

Publisher's Note Springer Nature remains neutral with regard to jurisdictional claims in published maps and institutional affiliations.